Wet/dry influence on behaviors of closed-cell polymeric cross-linked foams under static, dynamic and impact loads

Kaewunruen, Sakdirat; Ngamkhanong, Chayut; Papaelias, Mayorkinos; Roberts, Clive

DOI:
10.1016/j.conbuildmat.2018.08.052

Wet/dry influence on behaviors of closed-cell polymeric cross-linked foams under static, dynamic and impact loads

Kaewunruen, Sakdirat; Ngamkhanong, Chayut; Papaelias, Mayorkinos; Roberts, Clive

DOI:
10.1016/j.conbuildmat.2018.08.052

Wet/dry influence on behaviors of closed-cell polymeric cross-linked foams under static, dynamic and impact loads

Sakdirat Kaewunruen[1,2*], Chayut Ngamkhanong[1,2], Mayorkinos Papaelias[3], Clive Roberts[2]

[1] Department of Civil Engineering, The University of Birmingham, United Kingdom
[2] Birmingham Centre for Railway Research and Education, The University of Birmingham, United Kingdom
[3] School of Metallurgy and Materials, The University of Birmingham, United Kingdom

*Corresponding author

E-mail : s.kaewunruen@bham.ac.uk

Highlights

- The deflections of the submerged specimens are less than those in dry condition.
- The dynamic and impact stiffness of the materials in wet condition seems to be very high while the damping tends to be lower than those in dry condition
- The closed cell polymeric foam materials fit really well as a soft to medium bracket type of under ballast mat applications in railway track systems

Graphical Abstract:

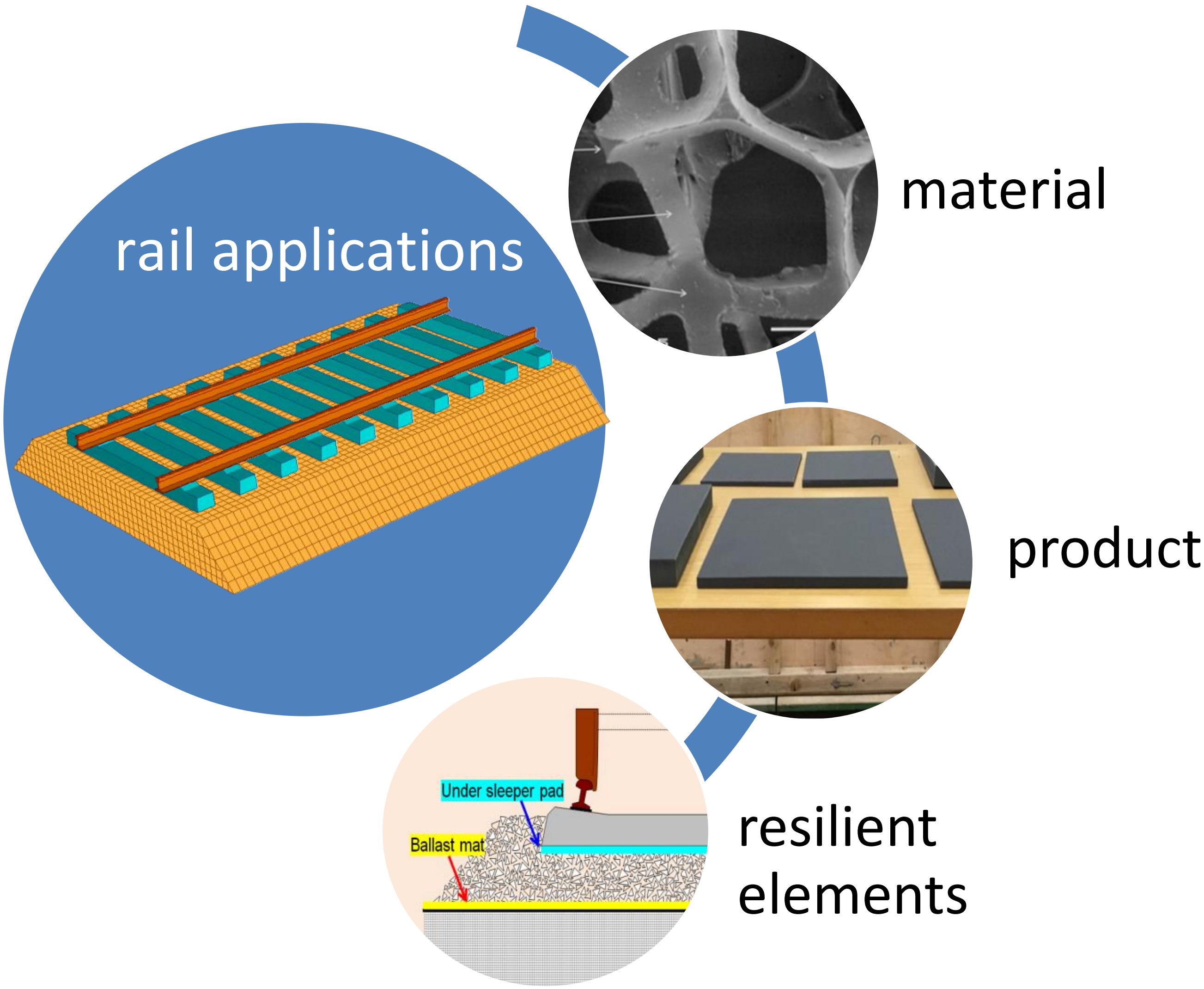
rail applications
material
product
Under sleeper pad
Ballast mat
resilient elements

Abstract

Polymeric materials have been used as critical components in a wide range of engineering structures in built environments. The superior characteristics of polymeric materials have led to various applications such as energy absorber during shock or impact events, lightweight structures, and thermal insulation. The key benefit is derived from relatively lower weight and density in comparison with other materials. The emphasis of this study is placed on closed-cell polymeric material, which is flexible and can potentially be manufactured as a rubber mat for railway track applications. A critical literature review reveals that the dynamic behavior of closed-cell polymeric material has not been fully investigated, especially when the materials are usually exposed to water. We are the first to present the wet/dry influences on the characteristics of closed cell cross-linked polyethylene foam under static, dynamic and shock loads. In our study, the water absorption and swelling of the materials are measured after 24 hours of immersion in de-ionized water. Static, dynamic, and impact loading are applied to closed-cell polymeric materials on both wet and dry states. The behaviors and responses of the materials can inform whether or not a closed-cell polymeric material can be used as under ballast mats and under sleeper pads in railway tracks under operational environments. Based on our results, it is found that this closed-cell-polymeric material is not suitable for use as under sleeper pads. However, they have reasonably strong potential for use as under ballast mats under various rail operational parameters.

Keywords: Polymeric foam, cross-linked polyethylene foam, water absorption, dynamic characteristics, under-ballast-mat, under-sleeper-pad

1. Introduction

Nowadays, polymeric materials have been widely used in a variety of applications in diverse industries such as insulated materials, vibration reduction device, clothing, application for protection, construction, automobiles etc [1-4]. The adventurous characteristics of the polymeric materials are the ease in material processing, high ductility, lightweight, thermal insulation, elastic wave barrier, etc. Polymeric foam materials are one of the most popular types of polymers as can be seen in all fields of daily life. The polymer foams used as a replacement of natural rubber were initially made in the 1930s [5]. Polymer foams are manufactured from a synthetic mix of solid and gas phase. Polymer foams can be characterized into open- or closed-cell structures by identifying their properties such as density, chemical properties, structure, and raw materials used. Naturally, open-cell foams are flexible, while closed-cell foams are relatively more rigid. The mechanical properties of foam are dependent on the type of polymer of which the cell walls are made of and their structure [6]. Also, the volume and amount ratio of open-cell to those of closed-cell is critical to establish strength of the foam. For closed-cell foams, the cells are surrounded by completed cell walls, which are isolated separately from each other. For open-cell foams, the cells are connected with each other. Hence, the advantages of open-cell foam are the softness, lightness, and inexpensiveness, while the closed-cell foams can gain more strength and have greater resistance to the leakage of air between the cells [7].

In terms of water absorption, the literature review reveals that closed-cell foams are imperative for preventing water penetration. On the other hand, the performance of open-cell polymeric materials can be deteriorated due to the high possibility of water absorption [8-10]. When the open-cell is surrounded by moisture environment, the open-cell foams tend to absorb more water and become an ineffective. Over recent decades, the dynamic behavior of polymer material under normal condition has been studied [11-15]. Nevertheless, the previous research has not considered the dynamic behavior of the polymeric material under wet condition.

The aim of this study is to highlight the influences of water absorption on closed-cell polymeric material under dynamic and impact loading. In addition, this is thus the world first to investigate the feasibility to use the closed-cell polymeric material as an under ballast mat and under sleeper pad in railway built environments. However, the use of under sleeper pad (USP) and under ballast mat (UBM) has spread over recent years but they have been used only on a case-by-case basis [16-19]. In practice, USP has been used predominantly to mitigate ballast breakage while UBM is often used to isolate ground-borne vibration and to moderate track stiffness at bridge, tunnels and stiffness transition zone. The findings from our investigations will help improve the understanding into material behaviors of closed-cell polymeric materials for real applications in railway track systems.

2. Material and methodology

2.1 Material

Fig 1 shows the comparison between typical microstructures of open- and closed-cell polymer foams, respectively. Complete cells can be seen in the interior of open-cell polymer foams. As can be seen from Figure 1a, all the cell faces are open so that air can pass freely between the cells of such foams. While in a typical closed-cell foams, each cell is surrounded by connected faces. Partial cells, with cut edges and faces, are obvious on the cut surfaces (Figure 1b), while complete cells exist in the interior of the sample. Although, the cell faces are thicker and stronger than those in closed-cell polymer foams, the cell faces can be split or otherwise damaged [7]. The polymer foams have been specially manufactured and supplied by Palziv Ltd., as part of an industry-based research project.

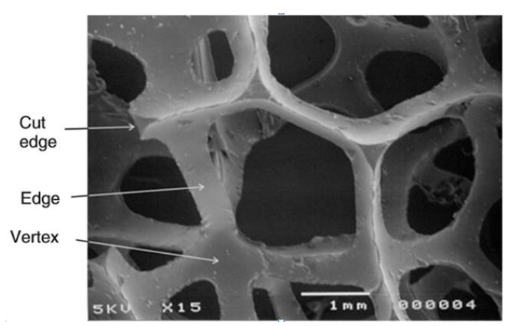

a)

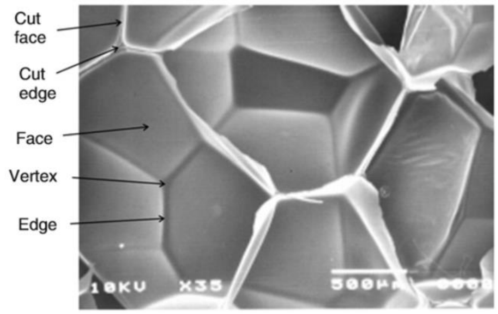

b)

Fig 1. SEM photograph of (a) PU open-cell foam of density 28kgm^{-3} (b) closed-cell low density polyethylene (LDPE) foam of density 24kgm^{-3} [7].

Polymer foam used as an elastic rubber mat is examined in this work. For a cube shape, solid mechanics' beam theorem can be applied. Young's modulus of the closed-cell foam can be calculated as follow [20]:

$$\frac{E_f}{E_s} \approx \varphi^2 \left(\frac{\rho_f}{\rho_s}\right)^2 + (1-\varphi)\frac{\rho_f}{\rho_s} + \frac{P_0(1-2v_f)}{E_S(1-\frac{\rho_f}{\rho_s})} \quad (1)$$

Where E_f is Young's modulus of foam, E_s is Young's modulus of polymer, φ is the mass fraction, ρ_f is the density of foam, ρ_s is the density of polymer, P_0 is the initial pressure of the gas contained in the foam cell, and v_f is Poisson ratio.

In terms of open-cell structure, for a cubic array of members, the beam theorem can also be adopted. The Young's modulus of open-cell foams become the term of relative density of the foam as follows [20]:

$$\frac{E_f}{E_s} = CR^2 \quad (2)$$

Where C is a constant, ≈ 1, and R is a relative density, ratio of the density of foam to the density of polymer. It is important to note that the elastic modulus of the open-cell foam tends to be solid when the relative density is close to one.

The polymeric material used in this study is block foam, which is a substance produced using plate-compressing technology. The polymeric material type used is hydrophilic polyurethane foam which has the density of 0.25 g/cm3. This material consist linear segmented block copolymers composted of hard and soft segments. The properties of this material include elasticity, transparency, low temperature performance, high resistance to abrasion, oil and grease. It is interesting to note that hydrophilic polyurethane foam acts like a sponge and can absorb the water and return to the original size [21]. Table 1 shows engineering characterization data for the polymer foam samples.

Table 1. Characterization data for the polymer foam samples.

Test	Standard	Result	Unit
Density	ISO 845	25	kg/m^3
Tensile strength MD*	ISO 1798	278	kPa
Tensile strength TD**	ISO 1798	209	kPa
Elongation MD	ISO1979	94	%
Elongation TD	ISO 1798	112	%
Compression 10%	ISO 844	17	kPa
Compression 25%	ISO 844	37	kPa
Compression 50%	ISO 844	96	kPa
Compression Set 25% 0.5H	ISO 1856	16.5	%
Compression Set 25% 24H	ISO 1856	9.5	%
Compression Set 50% 0.5H	ISO 1856	39	%
Compression Set 50% 24H	ISO 1856	30.5	%
Working Temperature Range	Palziv	-60 / 80	°C
Water Absorption %Vol (max)	Palziv	1	%
Water Vapour Transmission	ISO 1663	0.97	g/m^2 (24hrs)
Thermal Conductivity at 10°C	ASTM C177	0.039	W/mK
Thermal Conductivity at 40°C	ASTM C177	0.045	W/mK
Shore-OO	ASTM D2240	48	oo

*MD – Machine direction along the extruder's axis;
**TD – Transverse direction perpendicular to the extruder's axis.

The scanning electron microscope (SEM) was used to study the microstructure of this rubber by scanning electron microscope in to produce an image result from interaction between electron beam and atoms at various depths in the sample [22]. The test was carried out using Hitachi Tabletop Microscope TM3030, as shown in Fig 2a, at the School of Metallurgy and Materials, University of Birmingham. It is clearly seen that rubber mats used in this study are closed cell polymer foam, as shown in Fig 2b. The foam samples were specially manufactured and kindly supplied by the industry partner (Palziv). They were produced in an extrusion process. The dimensional stability of the sample over 24 hr at 70°C is less than 2%. It should be noted that the diameters of polymer foam are between 100 and 300 micron.

a)

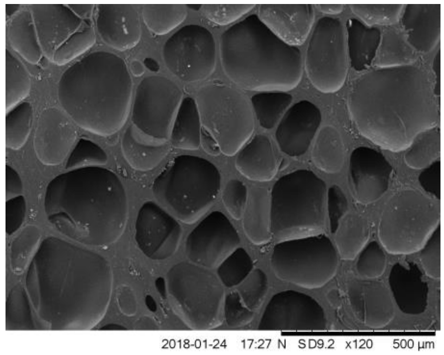

b)

Fig 2 a) Hitachi Tabletop Microscope TM3030 b) SEM photograph of closed-cell hydrophilic polyurethane foam

Polymer foam is primarily used in the following applications: packaging, automotive (cars, trucks, trains, etc.), toys, orthopedic products, brushes, car wash machines and other applications. In this study, polymer foam is used as a resilient material to study the feasibility of using polymer foam for practical applications in railway tracks such as under ballast mat and under sleeper pad.

The specimens (3 samples each) used for the water absorption and static tests were of the following dimensions:

i. 300 mm x 300 mm x 25 mm
ii. 300 mm x 300 mm x 10 mm
iii. 300 mm x 300 mm x 7 mm

In term of dynamic and modal testing, the specimens with the dimension of 100 mm x 100 mm were used. The specimens used are shown in Fig 3. In this study, there were four experiments. Firstly, water absorption analysis was used to find the percentage of absorption and the average swelling of polymer foam. After that, the wet and dry materials were used to compare the material properties including static behavior, dynamic behavior, and modal properties. All the tests were carried out at a control room temperature of 20 °C.

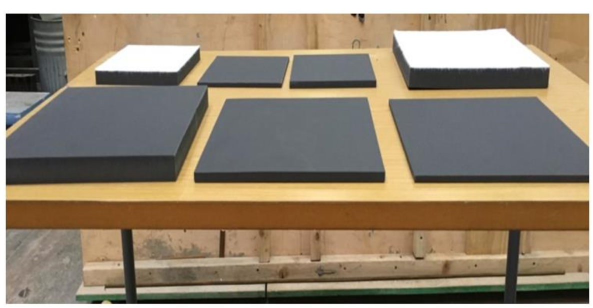

Fig 3. Polymer closed cell cross-linked foam

2.2 Water absorption analysis

The tests were carried out at the Department of Civil Engineering Laboratory at University of Birmingham, according to DIN 53428 [23] to determine the absorption of water by immersion for 1-day test period.

The area, weight and thickness of all three samples are measured. The samples are then submerged in water for 24 hours. The weight and thickness of the wet sample is calculated and the difference is noted to determine the water absorption rate and the swell behavior of the closed-cell polymer material.

The water absorption percentage of the sample is calculated by employing the following equation (3)

$$\textit{Water Absorption Percentage} = \frac{Wet\ Mass - Dry\ Mass}{Dry\ Mass}\ x\ 100 \tag{3}$$

The average swelling of the sample is calculated by using (4).

$$\textit{Average Swelling} = \textit{Average thickness of Wet Sample} - \textit{Average thickness of Dry Sample} \tag{4}$$

2.3 Static Testing

The tests were carried out using the Universal Testing Machine (UTM), Fig 4a, at the School of Mechanical Engineering Laboratory at University of Birmingham. The specimen was mounted on to the UTM, between steel plates of 300 mm x 300 mm dimensions, as shown in Fig 4b. Dry and wet specimens were subjected to static loading under vertical compression. The specimen was centrally fixed to the bottom steel plate to measure the static force made by the reaction force of the specimen to the top plate. The vertical displacements of the specimens were recorded while subjecting them to three cycles of 10 kN and 30 kN. It should be noted that the loading rates were defined as close as possible to its original thickness of specimen per minute, as noted in [24].

a)

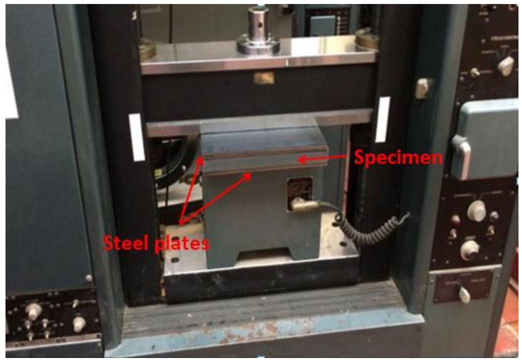

b)

Fig 4. a) Universal Testing Machine (UTM) b) Compression testing of specimen

2.4 Dynamic testing

The closed-cell polymer material samples with three thicknesses of (7, 10, 25 mm) with cross-sectional area of 100 x 100 mm^2 were compressed under cyclic loads using a dynamic compression machine (Fig 5). The dynamic cyclic pressures in between two stainless steel plates with the same loading area are simulated on the specimen stimulating the train passing over the rail segment. The test was conducted at the Metallurgy and Materials department at the University of Birmingham.

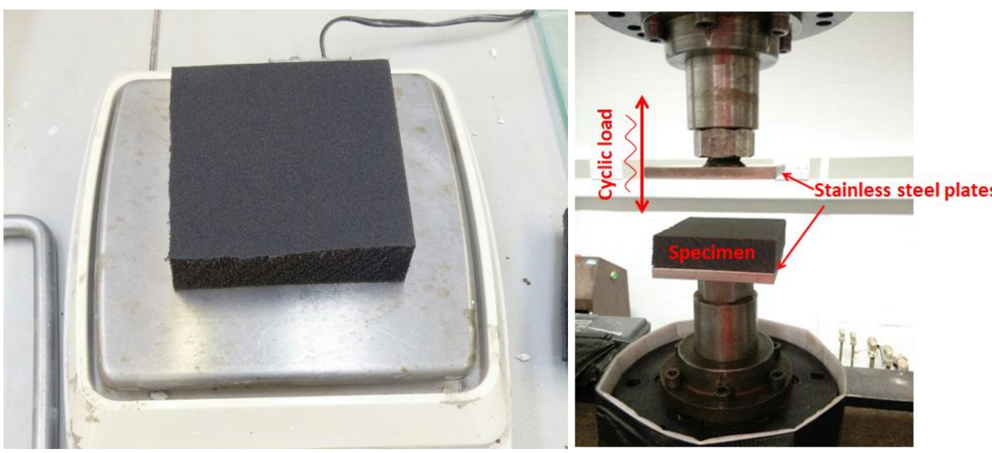

Fig 5. Specimen sample loaded into Dynamic Testing Machine

The experimental procedures were done to SBB standard (Swiss railway authority), consisting of a static pre-load of 0.6 kN (derived from a pre-load stress of 0.06 N/mm^2) and a sine function load of amplitude 0.3 mm (maximum safe displacement at testing frequencies) was applied at 1, 5, 10 and 20 Hz frequencies in order to calculate the frequency-dependent moduli of the material. The peak loading at each frequency was recorded to derive the dynamic bedding modulus (N/mm^3) as shown in equation (5).

$$Dynamic\ Bedding\ Modulus = \frac{Amplitude\ of\ Load\ (N)}{Maximum\ compression\ (mm)} \div Area\ of\ UBM\ (mm^2) \tag{5}$$

With respect to the load cell used to record the change in load, the sensitivity of the machine is 0.5 kN/V and therefore the peak-to-peak amplitude of the voltage change is equal to half of the amplitude of load.

2.5 Impact Modal Testing

Three sets of samples with different thicknesses (7, 10, 25 mm) and with the cross-sectional area of 100 x 100 mm^2 were setup for resonance testing using modal impact hammer (Fig 6). The sample was installed between two lumped steel masses. The base steel mass is pinned onto strong floor and the upper mass is free to generate a single degree of freedom (SDOF) movement as shown in Fig 7. The test was conducted at the Civil Engineering department at the University of Birmingham. The experimental procedures were done in accordance with the ISO standard for resonance testing [25]. The dynamic characteristics of the sample in the vertical direction can be described by the well-known equation of motion:

$$m_p\ddot{x} + c_p\dot{x} + k_p x = f(t) \tag{6}$$

$$\omega_n^2 = {}^{k_p}\!/_{m_p}, 2\zeta\omega_n = {}^{k_p}\!/_{m_p}, \zeta = {}^{c_p}\!/_{2\sqrt{k_p m_p}} \qquad \text{(7a, b, c)}$$

Where m_p, c_p, and k_p generally represent the effective rail mass, damping and stiffness of a rail pad, respectively. By taking the Fourier transformation of (6), the frequency response function can be determined. The magnitude of FRF is given by

$$H(\omega) = \frac{{}^{1}\!/_{m_p}}{\sqrt{(\omega_n^2 - \omega^2)^2 + (2\zeta\omega\omega_n)^2}} \tag{8}$$

Substituting equations (7) into equation (8) and using $\omega = 2\pi f$, the magnitude of the frequency response function $H(f)$ can be represented as follows:

$$H(f) = \frac{1}{m}\frac{4\pi^2\left(\frac{m}{k_p}\right)f^2}{\sqrt{\left[1 - 4\pi^2\left(\frac{m}{k_p}\right)f^2\right]^2 + \left[4\pi^2\left(\frac{m}{k_p}\right)\left(\frac{c_p^{\ 2}}{k_p m}\right)f^2\right]}} \tag{9}$$

where:

$H(f)$ = frequency response function (Nm/s^2)
f = loading frequency (Hz)
m = effective mass of rail or upper part (kg)
c_p = damping value of rail pad (Ns/m)
k_p = dynamic stiffness of rail pad (N/m)

Based on (9), these dynamic parameters can be extracted using modal testing measurements either in the laboratory or in the field.

Fig 6. Impact hammer and Prosig 8004 portable acquisition.

a) b)

Fig 7. a) SDOF dynamic modelling and b) Specimen sample under impact modal testing.

3. Results and discussions

3.1 Water absorption test

The experimental results of the water absorption test are tabulated in Table 2. The data are derived from the average of three samples in each set. It is noted that the foams with thickness of 25 mm absorb lesser water than the thin mats, while the 7mm has a highest percentage of water absorption. As for swelling, we observed that average swelling depend on the dimension and thickness. The larger dimension of under ballast mat can be swelled more than a smaller dimension due to larger surface area. When considering the volumetric effect, we note that the thinnest foams have the highest rate of swelling. However, the 25mm foams have the higher swelling rate than 10mm foams. Although the thicker closed cell cross-linked foams tend to have lesser permeability as seen in the water absorption results, some area of these foams may contain a little percentage of open cells which lead to the higher possibility of absorbing water.

Table 2. Water Absorption Test for polymer foam (24 Hours) – Absorption and Swelling Percentages.

Sample Thickness **(mm)**	Water Absorption Percentage (% by mass)	Swelling Percentage (% by volume)

7	**8.37 ± 1.04**	**1.86 ± 0.33**
10	**4.18 ± 0.39**	**0.57 ± 0.15**
25	**2.57 ± 0.16**	**0.90 ± 0.08**

3.2 Static testing

The static testing enables the analysis of static bedding modulus in order to evaluate the feasibility of using this closed cell foam materials in practice. The compression load-displacement and stiffness-compression load responses of dry specimens are shown from Figs 8a-8d, while the compression load-displacement and stiffness-compression load responses of specimens, submerged in water for 24 hours, are shown from Figs 8-9. According to load-displacement curves, it can be divided into two phases: elastic phase and densification phase. The loads increase rapidly with relatively small increase in displacement when closed-cell foams are compressed, the cell fluid or gas is also compressed and opposing cell walls come into contact which leads to an additional stress on the cell walls resulting in the densification phase. Since the polymer foam used is a low density material, it was noted that lower density foam indicated the higher degrees of densification [26]. On the other hand, the higher density foam exhibited lower strains at which densification began to occur. As for 10kN, displacement or strain remains almost the same in all cycles, which indicates that there would be no permanent strain and dissipated energy. However, when the load applied is higher resulting in the increase of compression strain, strain or displacement reaches its maximum value and the material cannot recover to its initial position. It is also noted that the area of hysteresis loop under load-displacement or stress-strain curve indicate energy dissipation of material. Thus, the energy dissipations increase with the increase in load and strain as observed in case of 30kN compression load. Hence, the foam has the irreversible losses over the first 2-3 cycles resulting in the slight reduction of moduli. It should be noted that bedding modulus is calculated using secant modulus.

Apparently, the modulus of submerged specimens is higher than the modulus of dry specimens. The bedding modulus, as shown in Table 3, is associated with the applications of the material as the resilient elements in railway tracks. It is noted that the modulus of this material is less than 0.1 N/mm^3 (which is the minimum stiffness requirement for the very soft under sleeper pads. Therefore, it is clear that this foam material cannot be applied as the under sleeper pads because the materials are too soft for such application. However, these foams can still be used in other industrial applications such as cushioning pads in packaging industry.

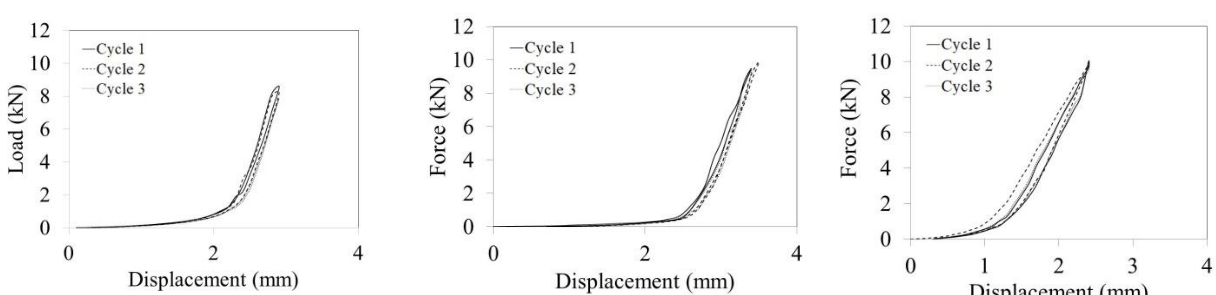

a) 300 x 300 x 7 mm b) 300 x 300 x 10 mm c) 300 x 300 x 25 mm

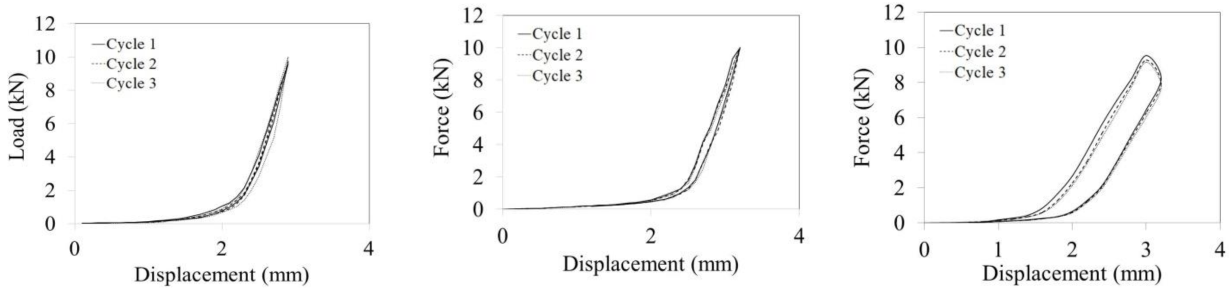

d) 300 x 300 x 7 mm (wet) e) 300 x 300 x 10 mm (wet) f) 300 x 300 x 25 mm (wet)

Fig 8. 10kN Load-displacement plots.

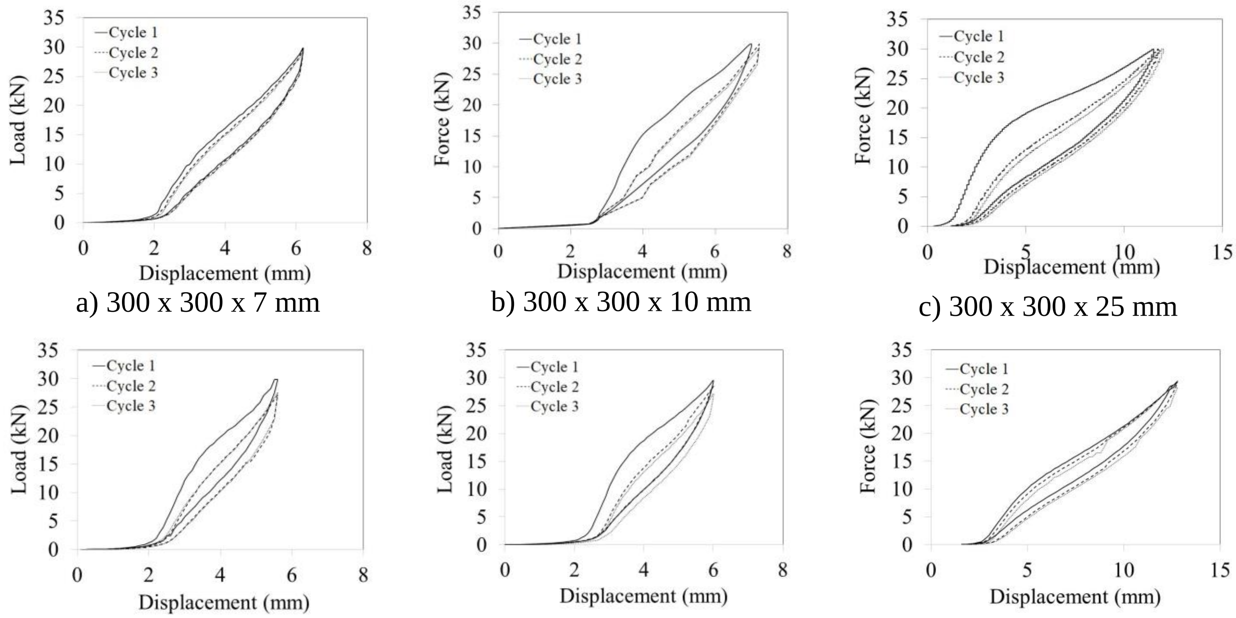

a) 300 x 300 x 7 mm b) 300 x 300 x 10 mm c) 300 x 300 x 25 mm

d) 300 x 300 x 7 mm (wet) e) 300 x 300 x 10 mm (wet) f) 300 x 300 x 25 mm (wet)

Fig 9. 30kN Load-displacement plots.

Table 3. Static moduli of materials.

Polymer foam thickness (mm)	at 10 kN preloading		at 30 kN preloading	
	Wet modulus (N/mm^3)	Dry modulus (N/mm^3)	Wet modulus (N/mm^3)	Dry modulus (N/mm^3)
7	0.037±0.001	0.032±0.002	0.056±0.003	0.053±0.002
10	0.035±0.001	0.031±0.002	0.053±0.003	0.047±0.001
25	0.034±0.001	0.030±0.001	0.046±0.003	0.036±0.012

3.3 Dynamic testing

As shown in Tables 4, the dynamic bedding moduli lie in the ranges of 0.09 – 0.22 N/mm^3. With respect to the stiffness categories set by SBB standards (by Swiss railway authority), the tested specimens are considered a ‘medium’ under ballast mat or ‘UBM’ (expected vertical deflection under a 225 kN load of between 0.5 – 1.0 mm), with the thicker 25 mm being one grade less stiff; the stiffness of 25 mm pads lie in the upper range of the 'Soft' UBM type with the vertical deflection being approximately 1.0 – 1.5 mm at the same loads. Fig 10 summarizes the frequency-dependent moduli of the material. Note that the vertical deflections of the specimens under wet condition are slightly lesser than those in dry condition. It is interesting to note that these results can further be validated by the static testing, where the static stiffness at 0 Hz are much lower than the stiffness at 1 Hz for all thicknesses of specimens. In addition, it is clear that the cross-linked foams have dynamic softening behavior: the thicker the foam, the softer the moduli.

Table 4. Results overview with derived stiffness of samples.

Thickness (mm)	Frequency (Hz)	Stiffness (N/mm^3)*		Sensitivity
		Dry	Wet	
7	1	0.133	0.140	0.5 kN/V
	5	0.143	0.151	
	10	0.149	0.156	
	20	0.151	0.159	
10	1	0.120	0.125	
	5	0.130	0.134	
	10	0.136	0.140	
	20	0.139	0.145	
25	1	0.073	0.075	
	5	0.079	0.082	
	10	0.083	0.086	
	20	0.086	0.089	

*standard deviations are less than 5%.

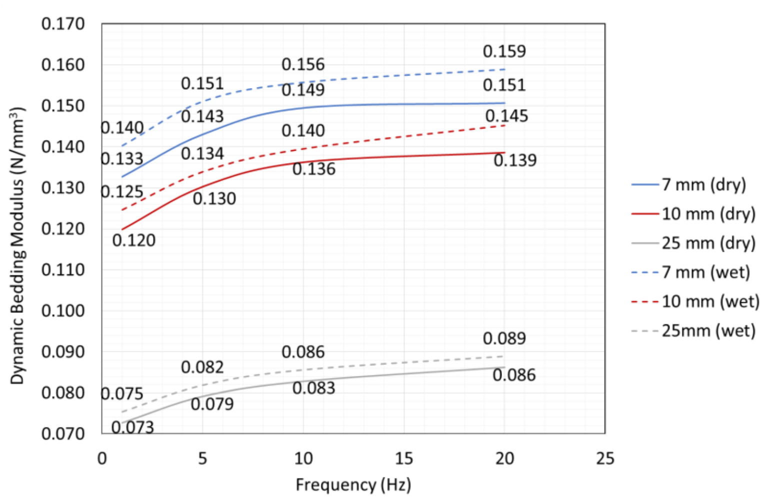

Fig 10. Frequency dependent moduli of samples.

3.4 Modal testing

The results of modal dynamic parameters can be obtained using a curve fitting method of SDOF vibration theory as demonstrated by Fig 11. The curve fitting method using DataFit is applied to the frequency response functions (FRFs) obtained from modal testing measurements to extract the effective mass, dynamic stiffness and damping of the polymeric foams. It should be noted that the correlation coefficients of curve fiting are less than 5%.Table 5 shows the summary of the impact modal parameters of the materials.

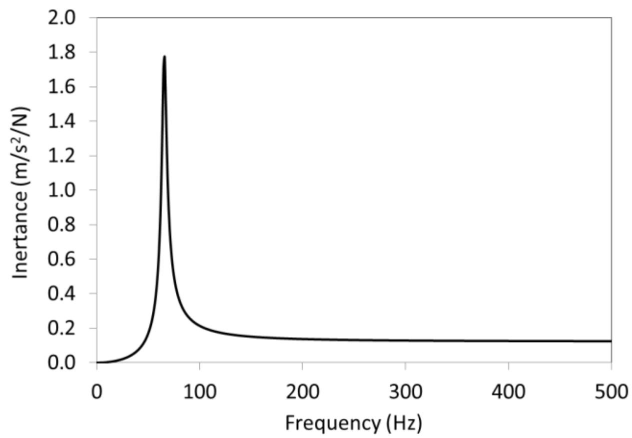

Fig 11. Best curve fitting to extract modal parameters (10 mm thickness in dry condition).

Table 5. Impact modal properties of materials.

Polymer Foam thickness (mm)	Dry			Wet		
	Moduli (N/mm^3)	Damping (Ns/m)	Resonant Frequency (Hz)	Moduli (N/mm^3)	Damping (Ns/m)	Resonant Frequency (Hz)
7	0.152	225	68	0.470	240	121
10	0.139	218	65	0.386	160	110
25	0.110	170	58	0.210	68	81

As can be seen from the Table 5, the material properties are changed by the water absorption. It is clear that the resonant frequencies and moduli increase when the foam cells absorb water, while damping tends to be lesser. Although damping constant of 7mm pad tends to be higher when it absorbs water, damping ratio is lesser due to the effect of moduli. This is clear from the solid mechanics perspective that the materials stiffen under impact pulse conditions. Also, the foams still maintain softening behavior under impact loading as the dynamic stiffness reduces with the thickness of material.

3.5 Feasibility study for UBM and USP applications of closed-cell polymeric materials

Railway tracks around the world suffer from the material deterioration, excessive noise and vibration, and differential settlements due to high-intensity dynamic impact load conditions generated at wheel and rail interface [27-29]. The impact load induced by train-track interaction can then exacerbate structural integrity of track components such as ballast, fastening system, sleepers and rails [30-38]. The deterioration of rail track geometry can also lead to poor ride quality and high stress threshold on train bogies and train couplers. Importantly, the cumulative damage of track components can undermine the safety of passengers. As a result, expensive and frequent maintenance of railway tracks can often be observed, especially at the location with impact damage of components such as ballast, formation and sleeper. In addition, the train speed might have to be reduced later due to the large track settlement in order to assure safe and comfort operations [39]. Such the speed penalty incurs service downtimes, delays and improvised train driving pattern, which can also cause other flow-on problems.

In order to reduce rapid track deterioration, special attention has been paid to the insertion of elastic layers in between track layers from rail foot to the top of formation. Fig 12 shows the feasible resilient insertion materials between component layers [40]. It was found that the insertions at rail and sleeper (i.e. rail pad and under sleeper pad) tend to dominantly improve the dynamic train-track interaction, while the resilient mat under ballast has very little effect on wheel/rail dynamics.

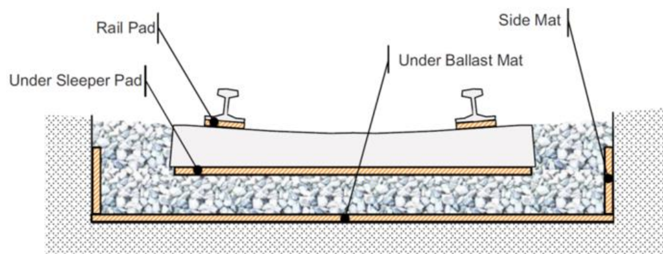

Fig 12. Feasible resilient insertion materials [13].

There are engineering guidelines regarding the appropriate use of the elastic layers, which have been developed by UIC [41]. The UIC Leaflet 179 presents the guideline for general USP usage, while UIC Code R-179-1 is the recommendations for UBM in ballasted tracks with a standard gauge. The code also provides information on the characterization of UBM such as mechanical characteristics, possible uses and some limitations.

3.5.1 Under ballast mat (UBM)

UBM can be applied in various operational environments such as conventional main lines, urban or high speed lines or light rail and metro lines. It is often been used in tunnels, bridges, elevated stations, underpasses, cuts, embankments, switches and railway stations. Different types of UBM are used for different locations and purposes. However, the main application of UBM is associated with vertical stiffness of the mat and tracks [42-46].

The UBM is characterized by the bedding modulus C (N/mm^3), that is to say the stiffness (N/mm) per unit area (mm^2) related to the area of the UBM situated under the ballast section (e.g. 1 bay of sleepers or 600 mm) that actually supports the load [47]. Table 6 shows the definition of very soft, soft, medium and hard UBM in relation to their dynamic bedding modulus C_{dyn}, with expected dynamic track vertical deflections under passing loads.

Table 6. UBM characterisation [40].

Type of UBM	Expected increase of the vertical track deflection up to 225 kN axle load (measurement [SBB]) mm[a]	Dynamic bedding modulus N/mm^3[bcde]

Very soft	1.5 – 2.0	$0.03 < C_{dyn} \leq 0.05$
Soft	1.0 – 1.5	$0.05 < C_{dyn} \leq 0.09$
Medium stiff	0.5 – 1.0	$0.09 < C_{dyn} \leq 0.22$
Stiff	≤ 0.5	$0.22 \leq C_{dyn}$

a. Measured with an SBB moving measuring car at 10 km/h (200 kN axle load "Einsenkungsmesswagan").
b. Estimated values for the dynamic bedding modulus C_{dyn} are only valid for very stiff foundations (e.g. concrete).
c. For sleepers with smaller dimensions the C_{dyn} are shifted towards higher values. Lower axle loads imply a shift of the reference dynamic bedding modulus towards lower values. In contrast, higher train speeds in principle require a higher UBM bedding modulus in order to control ballast destabilization phenomena.
d. SBB: with 0.06 N/mm^3 preload and ± 0.04 N/mm^3 load at 20 Hz, using a flat steel plate.
e. Lower C_{dyn} values are expected using a ballast plate.

The applications of UBM in relation to its characterization can be found in Table 7. It is found that the softer the UBM, the better the vibration reduction.

Table 7. UBM applications and characterisations.

Fields of application of UBM	UBM			
	Very soft	**Soft**	**Medium**	**Hard**
Vibration reduction and ground-borne noise				
Ballast breakage protection				
On existing structures with reduced ballast thickness				
Transition zones				

The uses of UBM in the field have showed that very soft UBM can cause ballast dilation and destabilization. As a result, very soft and soft UBM shall be avoided for high speed tracks. The combinations of UBM with USP or even soft rail pads are also not recommended in general. The negative consequences are highly likely to reduce lateral track resistance due to ballast destabilization. Therefore, the use of UBM in sharp-radius curves is not recommended at present, unless ballast wall is constructed.

3.5.2 Under sleeper pad (USP)

USP can also be applied in various operational environments such as conventional main lines, urban or high speed lines or light rail and metro lines. It is often used in ballasted tracks with concrete sleepers. Different types of USP can be used at different locations and for different purposes [48-53]. However, the main application of USP is associated with vertical stiffness optimization of overall rail tracks in order to reduce ballast breakage [54-58].

Again, the USP is characterized by the bedding modulus C (N/mm^3), that is to say the stiffness (N/mm) per unit area (mm^2) related to the area of the USP situated under the concrete sleeper block (e.g. 250 mm wide) that actually supports the load. Table 8 shows the definition of very soft, soft, medium and hard USP in relation to their static bedding modulus C_{stat}. It is noted that the relationship between static and dynamic bedding modulus differs depending on the material. Therefore, this classification is not exactly corresponding to the dynamic behavior of the track.

Table 8. USP characterisation [41].

Type of USP	Stiffness N/mm^3
Stiff	$0.25 < C_{stat} \leq 0.35$
Medium stiff	$0.15 < C_{stat} \leq 0.25$
Soft	$0.10 < C_{stat} \leq 0.15$
Very soft	$C_{stat} \leq 0.10$

The applications of USP in relation to its characterization can be found in Table 9. The recommendations are based on the experience on tracks with axle load ≤ 250 kN and speeds up to 300 km/h. There is little experience on higher axle load tests, but a trial has been in progress in Sydney Australia. At this stage, it is not clear if USP will generate positive influences on heavy haul rail networks.

The USP has different effects on lateral track resistance. It cannot be confirmed whether positive or negative effects will occur at this stage. However, USP can lead to excessive sleeper vibration, resulting in ballast dilation or ballast spreading. As such, special inspection and maintenance regime should be applied especially when using soft USP. The track degradation will further reduce the lateral track resistance. The longitudinal and lateral track resistance must be considered on a case by case basis, depending on the methodology of rail stress adjustment for continuous welded rail (CWR). Curve pull-in can incur if there is a loose of ballast and track support. The combination of USP and UBM can lead to unpredictable behavior of ballast and therefore such combination is not recommended. This negative influence also applies to the combination of USP with soft rail pads.

Table 9. USP applications and characterisations.

Fields of application of USP	USP			
	Very soft	Soft	Medium stiff	Stiff
Improve track quality (reduce ballast breakage and track/turnout pressure)				
Transition zones				
On existing structures with reduced ballast thickness				
Reduction of long-pitch low-rail corrugation in tight curves				
Reduction of ground-borne vibration				

3.5.3 Design specifications for USP / UBM

The uses of USP and UBM depend largely on the operational parameters (such as speed, axle load and services tonnage) and track parameters (stiffness, insertion loss, thickness of ballast, and existing support structure). Fig 13 shows the effectiveness of resilient layer in improving dynamic forces where P_1 is the high frequency dynamic force and P_2 is the lower frequency dynamic force [58].

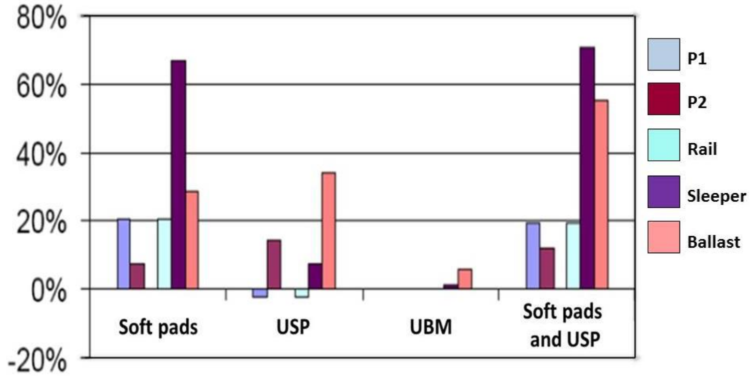

Fig 13. Reduction of dynamic wheel/rail forces using resilient materials [58-60].

3.5.4 Applications of closed cell cross-linked polymeric foam materials

Few types of resilient material have been kindly provided and then preliminarily evaluated for feasible applications as under-ballast mats in railway tracks. The materials have been assessed under static, dynamic and impulse loading conditions, in order to map their functionalities across the applications in rail operational environments.

1. Insight from static tests
   The materials tend to have a very low stiffness and bedding modulus. It is noted that the moduli of this material are in the ranges between 0.03 and 0.06 N/mm^3 as seen in table 3, while the minimum stiffness requirement for the very soft under sleeper pads is 0.1 N/m^3. Thus, they cannot be used as under sleeper pads.

2. Insight from dynamic tests
   The dynamic bedding moduli of 25mm pad lie in the range of 0.05 and 0.09 N/mm which is a soft UBM. It is interesting that both 7mm and 10mm fit as a medium UBM. The materials fit really well as a soft to medium bracket type of under ballast mat applications. According to table 7, the 25mm can be used on transition zones and on existing structure to reduce ballast thinkness, while 7mm and 10mm pads can be used for vibration reduction and ballast breakage reduction.

3. Insight from impact modal tests
   In wet condition, the dynamic stiffness of the materials seems to be very high while the damping tends to get lower than those in dry condition.

It is important to note that our experimental results reveal that the materials have strong potential for uses as under ballast mat in various applications as tabulated in Table 10 below.

Table 10. Applications of UBM.

Fields of application of UBM	**UBM**
Vibration reduction and ground-borne noise mitigation	25mm pad
Ballast breakage protection	25mm pad or 10mm pad

On existing structures with reduced ballast thickness	10mm pad
Stiffness transition zones (bridge end, turnout, slab tracks)	10mm pad or 7mm pad

It is recommended that further tests of the prototype UBM be carried out in details under laboratory conditions (with various temperatures) and under actual operational conditions to understand its behavior under train loads. However, the use of UBM tends to be fit for purpose and a field demonstration should be carried out before its commercialization. In the field experiments, the material could be installed on top of the formation and on top of bridge deck. Actual train services could be operated to yield a realistic field performance of the product.

4. Conclusion

In this study, closed cell cross-linked hydrophilic polyurethane foam materials, which are flexible with medium hard surface, are investigated for applications in civil construction and railway industries. There have been several studies focusing on behavior of closed-cell polymer foams. Nonetheless, the dynamic and impact behaviors of closed-cell polymeric foam material has not been thoroughly investigated, especially when the foam materials are exposed to water. This paper presents the influences of water absorption on closed-cell polymeric cross-linked foam materials under static, dynamic, and impact loading. Moreover, the feasibility to use polymer foams for rail track applications such as under-ballast mat, under-sleeper pad, is evaluated. After the samples are submerged in de-ionized water for 24 hours, it is interesting to note that 2.5-10% of water absorption and 0.5–2% of average swelling can be observed. The static and dynamic moduli of submerged specimens are more than the moduli of dry specimens. In addition, the deflections of the submerged specimens are less than those in dry condition. In wet condition, the dynamic and impact stiffness of the materials seems to be very high while the damping tends to be lower than those in dry condition. Moreover, material properties of the closed cell polymeric foams portray softening behavior when the thickness of foams increases elasticity of the material. The highlight of this paper is the functionality mapping of material performance across the applications in rail operational environments. The experiments exhibit that the closed cell polymeric foam materials fit really well as a soft to medium bracket type of under ballast mat applications in railway track systems. It is recommended that future tests include laboratory tests under various temperature conditions and field tests under actual operational conditions to understand its real behavior under train loads.

Acknowledgement

The project team would like to specially thank European Regional Development Fund (ERDF) for HiTech Rail Grant, which financially supports this research enabling commercial developments for small and medium enterprises in West Midlands. The technical support and specimens provided by u are highly appreciated. Not only can this research outcome benefit railway industry, but it has also provided strong business partnerships and significant impact to other industry, academia, and STEM education. We would like to sincerely thank European Commission for H2020-MSCA-RISE Project No. 691135 "RISEN: Rail Infrastructure Systems Engineering Network," which enables a global research network that tackles the grand challenge in railway infrastructure resilience and advanced sensing under extreme conditions (www.risen2rail.eu) [61].

Reference

[1] L.J. Gibson, M.F. Ashby, Cellular Solids: Structure and Properties., second ed., Oxford, 1997.

[2] N. Gardner, E. Wang E, P. Kumar, A. Shukla, Blast mitigation in a sandwich composite using graded core and polyurea interlayer, Exp Mech. 52(2) (2012) 119-133.

[3] B. Koohbor, A. Kidane, Design optimization of continuously and discretely graded foam materials for efficient energy absorption, Mater Des. 102 (2016) 151-161.

[4] R. Leszek, S. Milan. Modeling of non-elastic properties of polymeric foams used in sport helmets, procedia engineering. 177 (2017) 314-317.

[5] B. Otto, Das Di-Isocyanat-Polyadditionsverfahren (Polyurethane), Angewandte Chemie. 59 (1947) 257–288.

[6] S. Adamczak, J. Bochnia, B. Kaczmarska, An analysis of tensile test results to assess the innovation risk for an additive manufacturing technology, Metrology and Measurement Systems. 22(1) (2015) 127–138.

[7] N.J. Mills, Polymer Foams Handbook Engineering and Biomechanics Applications and Design Guide, 2007.

[8] A. Sabbahi, J.M. Vergnaud, Absorption of water at 100°C by polyurethane foam, Eur. Polym. J. 27 (1991) 845–850.

[9] A. Sabbahi, J.M. Vergnaud, Absorption by water by polyurethane foam: modelling and experiments, Eur. Polym. J. 29 (1993) 1243–1246.

[10] D.J. Gunn, D.R. Moores, W.J. Thomas, A.P. Wardle, Sorption of water vapour onto polyurethane foams, Chem. Eng. Sci. 29(2) (1974) 549–559.

[11] J. Zhang, N. Kikuchi, V. Li, A. Yee, G. Nusholtz, Constitutive modeling of polymeric foam material subjected to dynamic crash loading, Int. J. Impact Eng. 21(5) (1998) 369-386.

[12] M. Avalle, G. Belingardi, R. Montanini, Characterization of polymeric structural foams under compressive impact loading by means of energy-absorption diagram, Int. J. Impact Eng. 25(5) (2001) 455-472.

[13] S. Ouellet, S. Cronin, M. Worswick, Compressive response of polymeric foams under quasi-static, medium and high strain rate conditions, Polym. Test. 25(6) (2006) 731-743.

[14] S. Ouellet, D.S. Cronin, J. Moulton, E.O. Petel, High rate characterization of polymeric closed-cell foams: challenges related to size effects, Dynamic Behavior of Materials. 2013; 1 (2013) 21-28.

[15] B. Koohbor, A. Kidane, W.Y. Lu, Characterizing the constitutive response and energy absorption of rigid polymeric foams subjected to intermediate-velocity impact, Polymer Testing. 54 (2016) 48-58.

[16] M. Sol-Sánchez, F. Moreno-Navarro, M.C. Rubio-Gámez, The use of elastic elements in railway tracks: A state of the art review, Construction and Building Materials. 75 (2015) 293–305.

[17] L. Auersch, Dynamic axle loads on tracks with and without ballast mats, Proceedings of the Institution of Mechanical Engineers. 220(2) (2006) 169-183.

[18] S. Witt. The Influence of Under Sleeper Pads on Railway Track Dynamics. Department of Management and Engineering, Linköping University, 2008.

[19] R. Schilder. USP (UNDER SLEEPER PADS) – A CONTRIBUTION TO SAVE MONEY IN TRACK MAINTENANCE, AusRAIL PLUS, Sydney, AusRAIL PLUS, 2013.

[20] L.J. Gibson, M.F. Ashby, Cellular solids - Structure and properties (second edition), Cambridge University Press, 2001, ISBN 0-521-49911-9.

[21] Use of Hydrophobic and Hydrophilic Polyurethane Foams for Crack Injection, http://www.emecole.com/pages/Use-of-Hydrophobic-and-Hydrophilic-Polyurethane-Foams-for-Crack-Injection.html

[22] D.J. Stokes, Principles and Practice of Variable Pressure Environmental Scanning Electron Microscopy (VP-ESEM), Chichester: John Wiley & Sons, 2008.
[23] Deutsches Institut Fur Normung E.V. (German National Standard), DIN 53428, Determination of the behaviour of cellular plastics when exposed to fluids, vapours and solids, 1986.
[24] International Organization for Standardization, Rigid cellular plastics -- Determination of compression properties, ISO 844:2014, 2014.
[25] International Organization for Standardization, Methods for the calibration of vibration and shock transducers - Part 32: Resonance testing - Testing the frequency and the phase response of accelerometers by means of shock excitation, ISO 16063-32:2016, 2016.
[26] S.G. Kroeker, S.J. Bonin, A.L. DeMarco, C.A. Good, Age Does Not Affect the Material Properties of Expanded Polystyrene Liners in Field-Used Bicycle Helmets, Journal of Biomechanical Engineering, 138(4) (2016) 041005.
[27] D. Plotkin, D. Davis, Bridge approaches and track stiffness, Technical Report No DOT/FRA/ORD-08-01, Federal Railroad Authority, Washington DC, USA. 2008.
[28] A.M. Remennikov, S. Kaewunruen, A review of loading conditions for railway track structures due to train and track vertical interaction, Structural Control and Health Monitoring. 15(2): 207-234.
[29] S. Kaewunrune, Impact Damage Mechanism and Mitigation by Ballast Bonding at Railway Bridge Ends, International Journal of Railway Technology (2014) 1-22.
[30] R. Gustavson, Structural behaviour of concrete railway sleepers, Chalmers University of Technology, Department of Applied Mechanics., 2002.
[31] S. Kaewunruen, A.M. Remennikov, Effect of improper ballast packing /tamping on dynamic behaviours of on-track railway concrete sleeper, International Journal of Structural Stability and Dynamics. 7(1) (2007) 167-177.
[32] S. Kaewunruen, A.M. Remennikov, Experimental simulation of the railway ballast by resilient materials and its verification by modal testing. Experimental Techniques 32(4) (2008) 29-35.
[33] A.M. Remennikov, S. Kaewunruen, Experimental load rating of aged railway concrete sleepers, Engineering Structures. 76(1) (2014) 147-162.
[34] S. Kaewunruen, A.M. Remennikov, Nonlinear transient analysis of a railway concrete sleeper in a track system, International Journal of Structural Stability and Dynamics. 8(3) (2008) 505-520.
[35] S. Kaewunruen, A.M. Remennikov, Dynamic flexural influence on a railway concrete sleeper in track system due to a single wheel impact, Engineering Failure Analysis. 16(3) (2009) 705-712.
[36] S. Kaewunruen, A.M. Remennikov, Effect of a large asymmetrical wheel burden on flexural response and failure of railway concrete sleepers in track systems, Engineering Failure Analysis. 15(8) (2008) 1065-1075.
[37] S. Kaewunruen, A.M. Remennikov, Nonlinear finite element modeling of railway prestressed concrete sleeper, Proceedings of the 10th East Asia-Pacific Conference on Structural Engineering and Construction. 4 (2006) 323-328.
[38] C. Ngamkhanong, S. Kaewunruen, C. Baniotopoulos, A review on modelling and monitoring of railway ballast. Structural Monitoring and Maintenance 4(3) (2017) 195-220.
[39] J. Kennedy, P.K. Woodward, G. Medero, M. Banimahd, Reducing railway track settlement using three-dimensional polyurethane polymer reinforcement of the ballast, Construction and Building Materials. 44 (2013) 615-625.
[40] International Union of Railway, UIC Recommendation R917-1 Under ballast mat, Paris, France, 2011.
[41] International Union of Railway. UIC Leaflet 917 Guidelines for under sleeper pad, Paris, France, 2015.
[42] P. Teixeira., State-of-the-Art on the use of bituminous subballast on european high-speed rail lines, Congress of bearing capacity of roads, railways and airfields, Barcelona, Spain, 2009.
[43] S. Potocan, Ballast mats within areas of reduced ballast depth, European railway review. 5 (2010).

[44] Y. Kimura, Control of ground-borne vibration from at-grade track using ballast mats, Proceedings of American public transit association rapid transit conference. 1995.

[45] S.F. Brown, B.V. Brodrick, N.H Thom, and McDowell, The Nottingham railway test facility. In: Proceedings of the Institution of Civil Engineers – Transport. 2007.

[46] G. Werkstoffe, Ballast mats. Characteristics of solutions in service, Paris, UIC, 2006

[47] International Union of Railway, UIC Code 719-83 Recommendations for the use of under ballast mats, 1st ed., VII Way and Works, 2011.

[48] A. Johansson, J.C.O. Nielsen, R. Bolmsvik, A. Karlström, Under sleeper pads – influence on dynamic train-track interaction, Wear. 265 (2008) 1479–687.

[49] International Union of Railway, USP Report, Under sleeper pads, Project no. I/05/U/440, Summarising report, 2009.

[50] International Union of Railway, USP recommendations, Under Sleeper Pads, Recommendations for Use, UIC-Leaflet, Draft Document, 2013.

[51] R. Schilder, UIC project no. I/05/U/440 USP-under sleeper pads, Applications and benefits of elastic elements in ballasted tracks UIC, Paris 17, 2006.

[52] J. Jenkins, S. Stephenson, G. Clayton, G. Morland, D.L. Lyon, Incidences des paramètres caracteristiques de la voie et des vehicules sur les efforts dynamics verticaux qui se développent entre rail et roue, Rail International. 3(10) (1974) 682-702.

[53] S. Lakuši, M. Ahac, I. Haladin, Experimental investigation of railway track with under sleeper pad, 10th Slovenian road and transportation congress. Portorozˇ, Slovenija, 20(2) (2010).

[54] T. Dahlberg, Railway track stiffness variations-consequences and countermeasures, Int. J. Civ. Eng. 8(1) (2010) 1–12.

[55] P. Schneider, R. Bolmsvik, J.C.O. Nielsen, In situ performance of a ballasted railway track with under sleeper pads, J. Rail Rapid Transit. 225(3) (2011) 299-309.

[56] W. Stahl, Improvement of ballasted tracks using sleeper pads – investigations and experiences in Germany Munich University of Technology, 2004.

[57] F. Müller-Boruttau, U. Kleinert , Betonschwellen mit elastischer Sohle, ETR. 2001 50(3) (2001).

[58] V.L. Marine, M.J.M.M. Steenburgen, I.Y. Sheets, Combating RCF on switch points by tuning elastic track properties, Wear. 271(1) (2009) 158-167.

[59] S. Kaewunruen, Monitoring structural deterioration of railway turnout systems via dynamic wheel/rail interaction, Case Studies in Nondestructive Testing and Evaluation 1 (2014), 19-24.

[60] S Kaewunruen, M Sechet, M Hamarat, K Goto, Life cycle evaluation of railway turnout crossings' impact attenuation methods using soft fasteners and composite sleepers, Proceedings of the Institute of Acoustics, 40 (2018) 97-105.

[61] S. Kaewunruen, M.J. Sussman, M Akira, Grand Challenges in Transportation and Transit Systems. Frontiers in Built Environment 2 (2016).